frontiers | Frontiers in Materials

TYPE Original Research
PUBLISHED 15 September 2022
DOI 10.3389/fmats.2022.992984

OPEN ACCESS

EDITED BY
Wenliang Li,
Jilin Medical University, China

REVIEWED BY
Tang Jiwei,
Shanghai Jiao Tong University, China
Xixiang Yang,
National University of Defense Technology, China

*CORRESPONDENCE
Jing Lv,
stunner2006@126.com

†These authors have contributed equally to this work and share first authorship

SPECIALTY SECTION
This article was submitted to Polymeric and Composite Materials, a section of the journal Frontiers in Materials

RECEIVED 13 July 2022
ACCEPTED 17 August 2022
PUBLISHED 15 September 2022

CITATION
Lv J, Zhou Y, Zhang Y, Nie Y and Wang Q (2022), Study of performance of aerostat envelope materials on the coast.
Front. Mater. 9:992984.
doi: 10.3389/fmats.2022.992984

Study of performance of aerostat envelope materials on the coast

Jing Lv[1*†], Yan Zhou[2†], Yuanping Zhang[1], Ying Nie[1] and Qian Wang[1]

[1]Aerospace Information Research Institute, Chinese Academy of Sciences, Beijing, China, [2]Changchun Institute of Applied Chemistry, Chinese Academy of Sciences, Changchun, China

In this article, the performance of several naturally aged envelope materials in Hainan, China, was studied. The results show that the outer layer contributes to the properties of the envelope materials, where PVF and PVDF are better candidates for a weathering layer than TPU and aluminum. Due to the superior water and mildew resistance of PVF and PVDF, the loss of tensile strength for 3216LV and FV1175 was slight, whose value reduced from 101.43 ± 5.45 Kgf/cm and 76.15 ± 3.81 Kgf/cm to 79.73 ± 6.40 Kgf/cm and 70.20 ± 6.57 Kgf/cm, respectively, when aging for 24 months with the helium permeability reduction from 0.8818 L/m^2•day•atm and 0.6360 L/m^2•day•atm to 0.2047 L/m^2•day•atm and 0.2169 L/m^2•day•atm aging for 18 months, in the case of FV1175 showed leakage after aging for 24 months due to delamination. However, the tensile strength of HV150 dropped from 82.13 ± 3.61 Kgf/cm to 15.22 ± 2.16 Kgf/cm at 24 months with helium leakage, owing to heavy mildew and degradation. Meanwhile, ETAV150 also exhibited a decreased tensile strength of 57.92 ± 1.32 Kgf/cm after 6 months aging, 32.8% lower than that of the original sample, and showed leakage when aging for 12 months. This research provides a theoretical guidance for the structural design and screen of envelope materials for aerostat used along the coast.

KEYWORDS

envelope materials, mechanical properties, helium permeability, natural aging, aerostat, along coast

Introduction

Lighter than air aerostats, including tethered balloons and stratospheric airships (Tang et al., 2021; Tang et al., 2019), serve as strategic equipment for reconnaissance, ocean observations, meteorological research, geological mapping, environmental protection, and so on (Schäfer et al., 2002; Liao and Pasternak, 2009). These numerous merits include a high-flying altitude, long stay in the air, strong survivability, wide coverage, and low cost of manufacture, operation, and maintenance, which render it an alternative and a complement to orbiting satellites (Shah et al., 2018). The envelope materials for aerostat must have low density, high strength, excellent weathering, low helium permeability, good stitching process, and easy repair, among other features (Schäfer et al., 2002; Kang et al., 2006; Komatsu et al., 2003), which are of vital significance due to their complex, changeable, and even harsh working

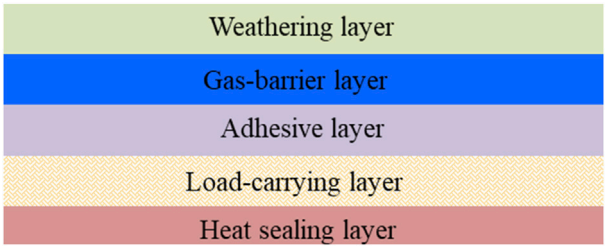

FIGURE 1
Typical laminated structure of envelope material for aerostat.

conditions (Cicerone, 1987; Caldwell and Flint, 1994; Wrobel et al., 2011). In addition to the application efficiency of the aerostat containing floating height and continuous flight time, the payload and the lifetime directly depend on the properties of the envelope materials (Meng et al., 2016; Meng et al., 2017).

To satisfy the these requirements, envelope materials for aerostat are laminates designed, typically including heat-sealing layer, load-carrying layer made of fabric, gas-barrier layer, weathering layer, and adhesive layers (Schäfer et al., 2002; Meng et al., 2017; Vallabh et al., 2021), as shown in Figure 1. The functional load-carrying layer, usually woven from aromatic polyamide (Vectran), polyester, polyethylene, and poly-p-phenylenebenzobisthiazole fiber, provides the strength of the whole envelope materials to bear the load, as well as the pressure difference between the inside and outside of aerostat (Komatsu et al., 2003; Zhai and Euler, 2005; Nakadate et al., 2009). The most critical part is the gas-barrier layer upon the load-carrying layer, which matters for the helium loss, cost, and hence the operation time of the aerostat. Typically used materials mainly include polyester (PET), ethylene vinyl alcohol copolymer, and polyvinylidene chloride (Gao et al., 2016). In addition, these layers cannot function for a long time without the protection of the

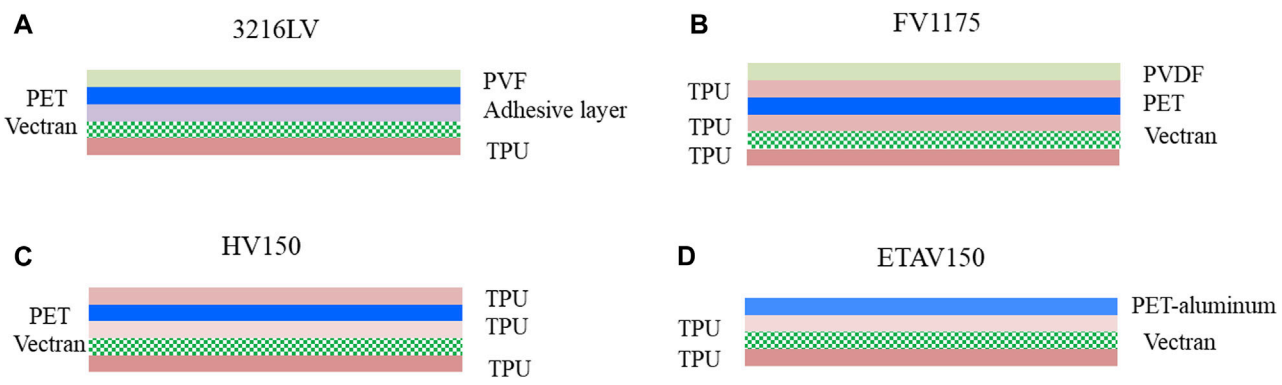

FIGURE 2
Structure of envelope materials. **(A)** 3216LV, **(B)** FV1175, **(C)** HV150, and **(D)** ETAV150.

TABLE 1 Representative meteorological data.

Date	T (°C)	RH (%)	Irradiation (MJ/m^2)	Date	T (°C)	RH(%)	Irradiation (MJ/m^2)
18/7/25	27.5	89.7	15.1	19/7/25	28.2	84.7	12.1
18/8/25	26.7	98.9	12.0	19/8/25	27.8	90.7	14.0
18/9/25	25.5	99.9	18.4	19/9/25	26.4	85.5	12.1
18/10/25	26.5	89.2	13.9	19/10/25	25.2	92.7	8.0
18/11/25	20.9	95.5	3.6	19/11/25	22.8	88.0	11.4
18/12/25	21.5	95.8	8.7	19/12/25	22.0	86.3	5.7
19/1/25	20.4	83.6	8.8	20/1/25	22.5	85.5	10.8
19/2/25	21.1	95.2	9.9	20/2/25	21.1	85.2	18.4
19/3/25	21.6	97.7	5.9	20/3/25	25.7	82.8	12.2
19/4/25	28.6	85.3	19.1	20/4/25	19.7	99.4	2.1
19/5/25	28.3	84.8	13.0	20/5/25	31.7	71.5	18.4
19/6/25	28.9	89.2	10.2	20/6/25	31.7	68.7	12.2

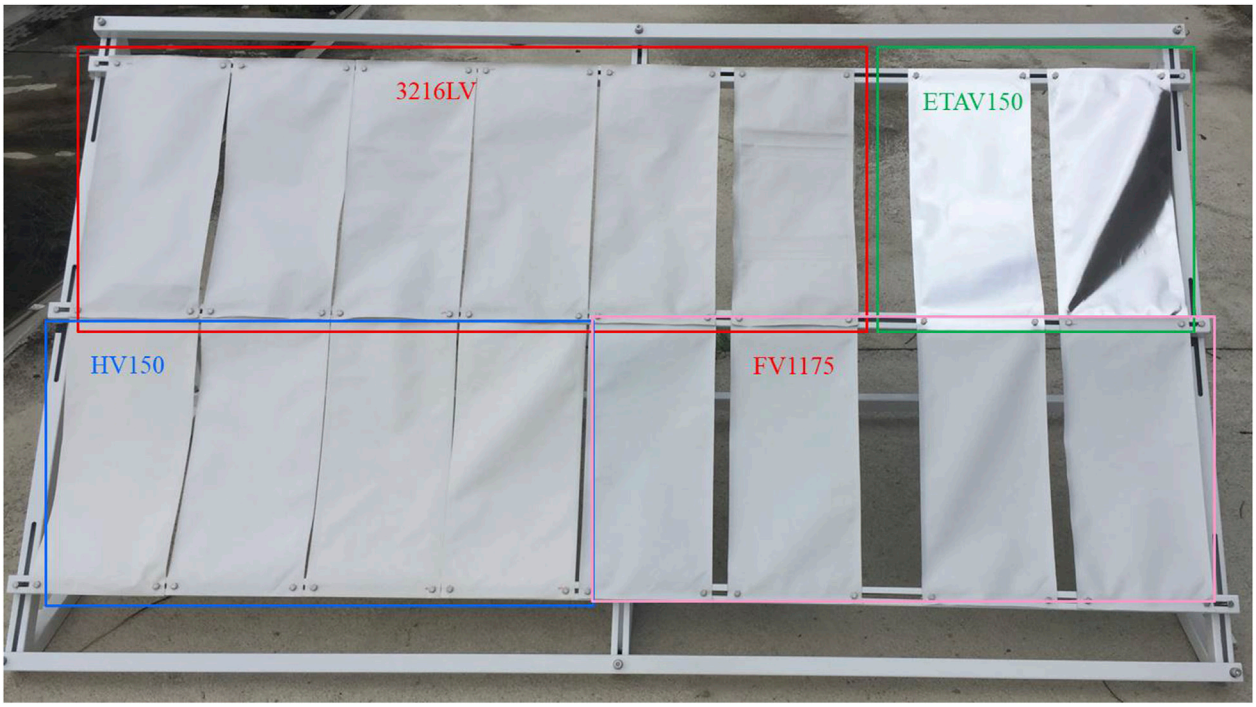

FIGURE 3
Natural aging tests of envelope materials.

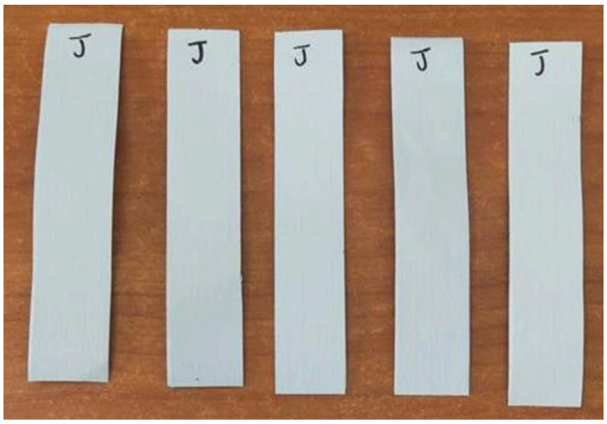

FIGURE 4
Tensile specimen and its schematic illustration.

weathering layer, which possesses extraordinary UV-blocking properties, serving as the outermost part of the aerostat envelope material. The weathering layer usually contains polyvinyl fluoride (PVF), polyvinylidene fluoride (PVDF), and polyurethane (TPU), with nanoparticles or an aluminized layer, which could prevent the inner layers from solar irradiation as well as other harms and hence guarantee the service life of the envelope materials as a whole (Razak et al., 2004). Adhesive layers are included to solve the poor interaction and low compatibility between functional layers (Baldan, 2004).

The dwell time for an aerostat is up to the performance of envelope materials, which is influenced by many factors, including the characteristics of the components of each layer, the laminated structure, and the working environment. Many experimental tests and theoretical simulations have been conducted to better understand the influence mechanism of these factors on the properties of envelope materials (Garg et al., 2011; Qu et al., 2019; Shi et al., 2018; Wang et al., 2017). Garg et al. (2011) found that helium permeation limits the endurance by affecting the ability of the airship against the impact of gushes and by increasing the total weight of the airship. Meng et al. (2016; 2017) and Qu et al. (2019) investigated the microscopic tear propagation and fatigue damage mechanism of envelope materials and established related test criteria in combination with analytical models. Kang et al. (2006) developed a CAD model and characterized the static properties of envelope materials consisting of helium barrier, load-carrier, and thermal bonding layer, finding that the high stiffness and strength of Vectran-based envelope materials possess wide-

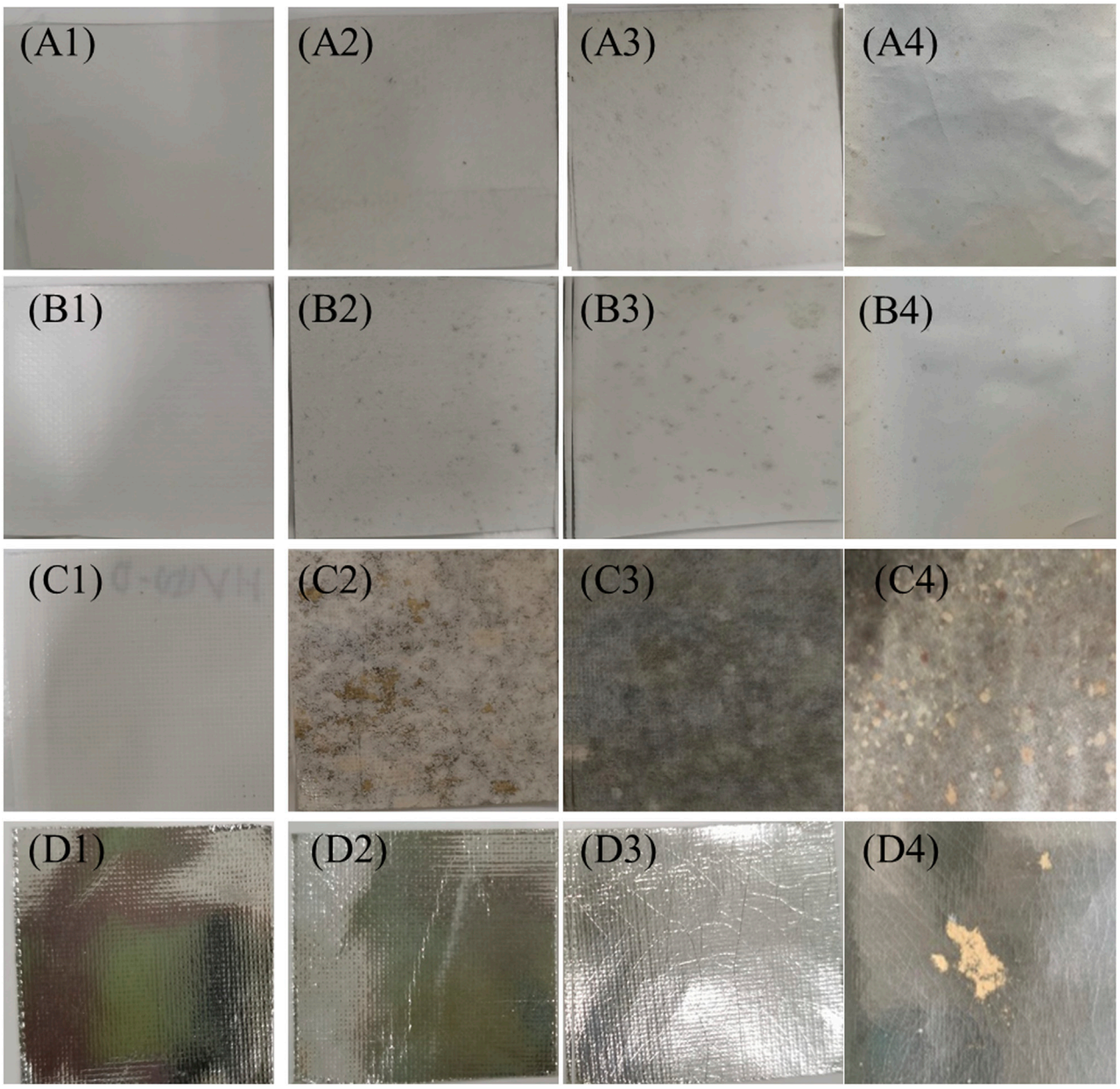

FIGURE 5
Images of envelope materials. **(A1–A4)** 3216LV, **(B1–B4)** FV1175, **(C1–C4)** HV150 aging for 0, 12, and 24 months, and number 4 is a local amplification of aging 24 months, and **(D1–D4)** ETAV150 aging for 0, 6, and 12 months, and number 4 is a local amplification of aging 12 months.

ranging temperature applicability, from −75 to 65°C. Vallabh et al. (2021) proposed a novel design concept using fiber-reinforced non-woven fabrics as load-bearing layer with EVOH and a vacuum-deposited aluminum-coated corrosion resistance layer for the envelope of high-altitude airships.

In addition, working or storage conditions, which receive little attention, also play critical roles in the service of envelope materials for airships (Lv et al., 2020). In our previous study, it was found that the hot-pressing temperature and flexing during processing as well as storing and utilization conditions contribute to mechanical properties and helium permeability (Lv et al., 2020). Among other factors, samples recovered from an actual flight on a stratospheric airship showed significantly reduced mechanical properties and even helium leakage due to excess solar irradiation, ozone concentration, and interaction of energetic particles. Thus, the working conditions are of vital significance. Predicting the properties of envelope materials in

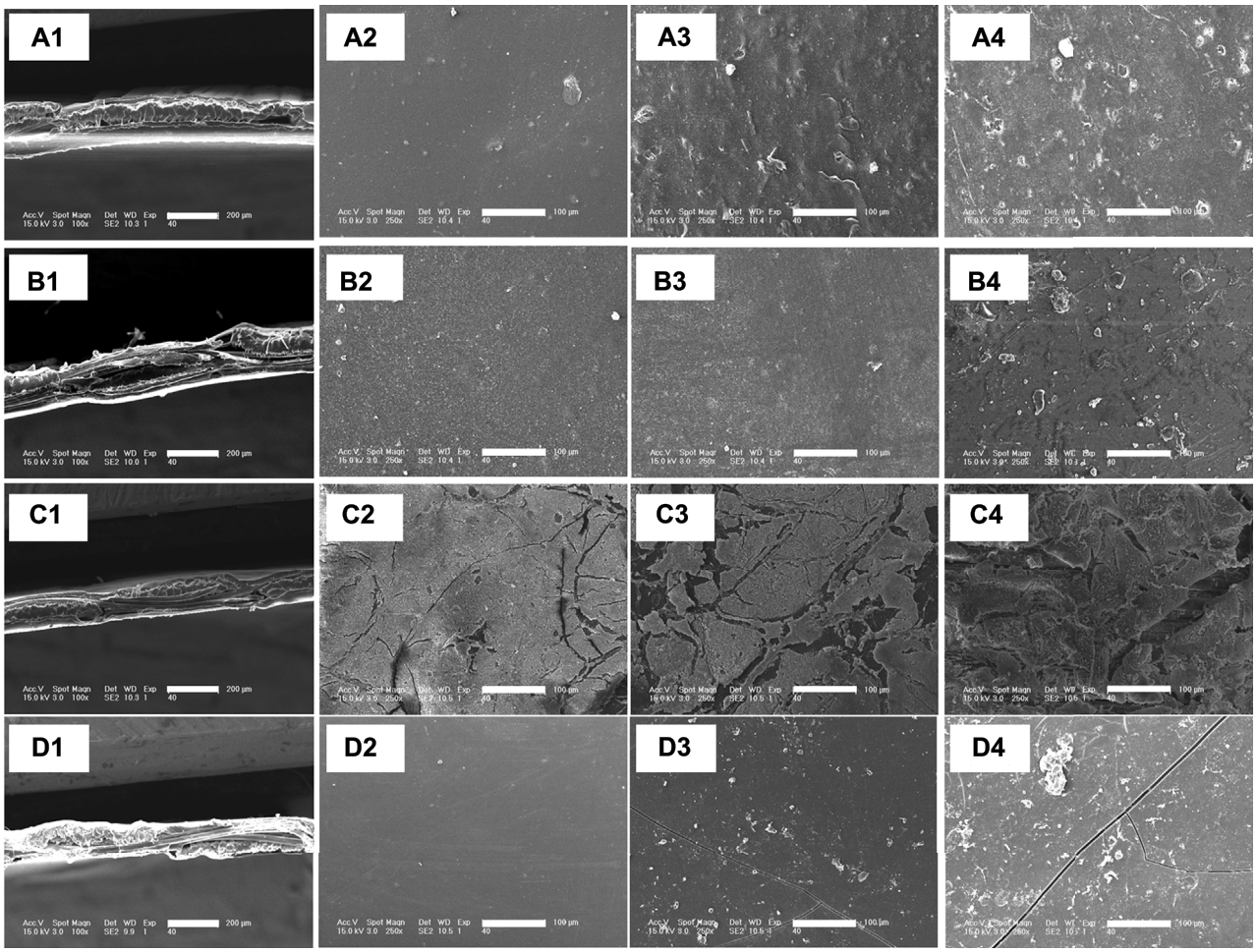

FIGURE 6
SEM images of **(A1–A4)** 3216LV, **(B1–B4)** FV1175, **(C1–C4)** HV150 (numbers 1 and 2 show the section and surface morphology of original sample, numbers 3 and 4 show the sample aging for 12 and 24 months), and **(D1–D4)** ETAV150 (numbers 1 and 2 show the section and surface morphology of original sample, numbers 3 and 4 show the sample aging for 6 and 12 months).

TABLE 2 Weight changes of envelope materials before and after immersing in deionized water.

Weight (g)	3216LV	FV1175	HV150	ETAV150
before	1.9249	1.7654	1.7326	1.8941
after	1.9247	1.7635	1.6987	1.8684
change	−0.0002	−0.0019	−0.0339	−0.0257

the working environment can provide guidance for choosing and designing materials to meet requirements. However, it is costly, time-consuming, and laborious to assess the performance for envelope materials through assembling envelope materials into airships and flying into the stratosphere. Therefore, outdoor aging experiments are more favorable.

Ocean area accounts for 71% of the earth's surface. Much work should be performed on the sea, such as meteorological monitoring and military cruises, that can be conducted by the aerostat. Hence, the performance of envelope stored or working along or on the sea due to its high salt and moisture, making it distinct from working on land, matters greatly (Conrads, et al., 2010). In this article, four types of envelope materials for aerostat aged in Hainan, China, a coastal city, and properties were tested. The results show that envelope materials with an aluminizing and TPU weathering protection layer is not applicable in Hainan with its high moisture content. Thus, there is better performance for envelope materials with PVF and PVDF as a weathering layer. These results have significance for selecting or designing envelope materials for aerostats utilized along coast or on the sea.

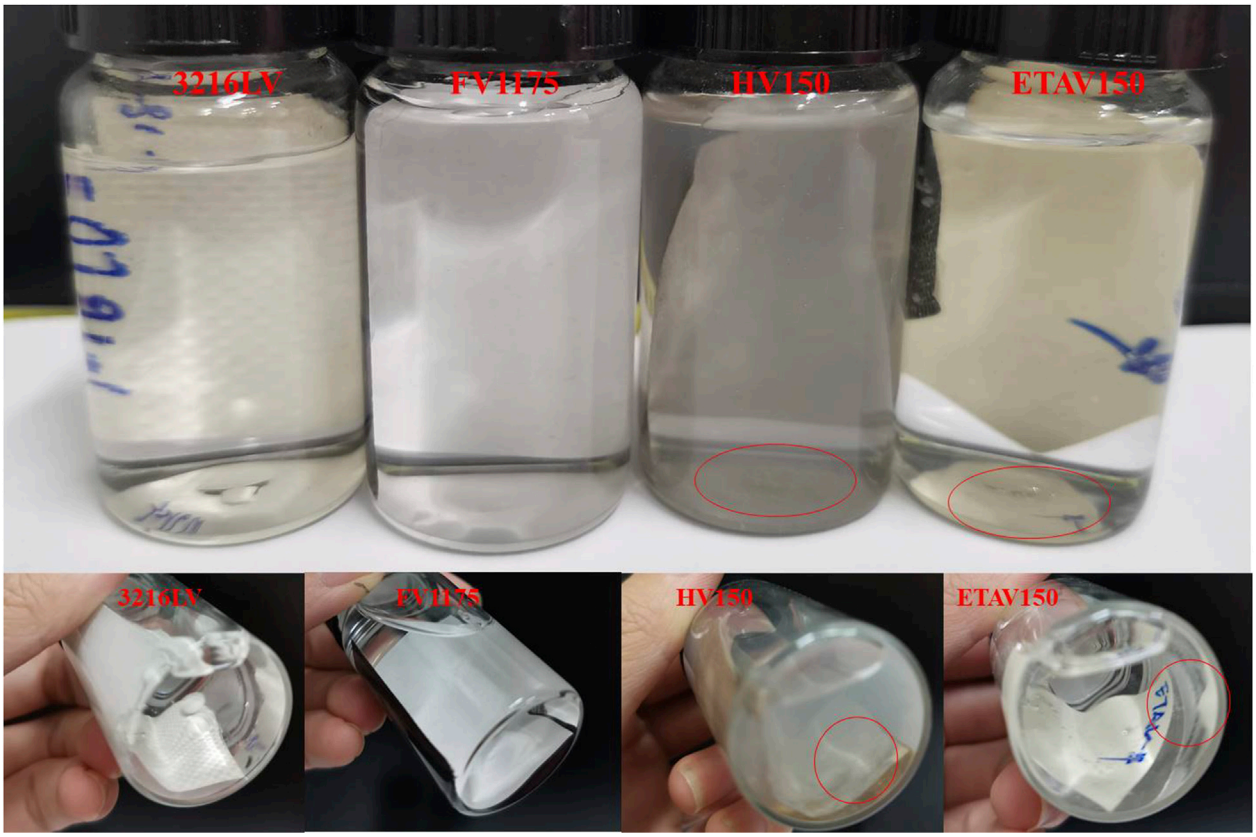

FIGURE 7
Images of aged 3216LV, FV1175, HV150, and ETAV150 soaked in deionized water (ETAV150 was aged for 12 months, and the others were aged for 24 months).

Experiments

Materials

Four types of envelope materials for aerostat, namely, 3216LV, purchased from Uretek, and FV1175, HV150, and ETAV150 provided by Changchun Institute of Applied Chemistry, were aged and analyzed in Hainan, China. The structures of these materials are shown in Figure 2: 3216LV, FV1175, HV150, and ETAV150 are composed of PVF/PET/adhesive layer/Vectran/TPU, PVDF/TPU/PET/TPU/Vectran/TPU, TPU/PET/TPU/Vectran/TPU, and PET-aluminum/TPU/Vectran/TPU, respectively. PET acts as a gas-barrier for 3216LV, FV1175, and HV150, where PVF, PVDF, and TPU with TiO_2 form the weathering layers, respectively. PET-aluminum worked as both weathering and gas-barrier layer in ETAV150.

Aging experiment

Natural aging tests were performed on the roof of a building with a height of 12 m in the open air, following ASTM G7-2013, in Danzhou, Hainan. As shown in Figure 3, pieces of envelope materials were placed on the natural aging frame outdoors at an angle of 45° for 24 months (July 20, 2018, to July 21, 2020, in Danzhou), with an average temperature, RH, daily accumulated irradiation, and annual cumulative rainfall above 20°C, 80%, and 840 mm, respectively. Concentrated high temperature, high humidity, and heavy rainfall occur during June to August with average temperature, RH, and annual cumulative rainfall of 28°C, 95%, and 1180 mm, respectively. The representative data are listed in Table 1. The samples were tested after aging for 6, 12, 18, and 24 months. The natural aging test was stopped after 12 months for ETAV150 because of helium leakage.

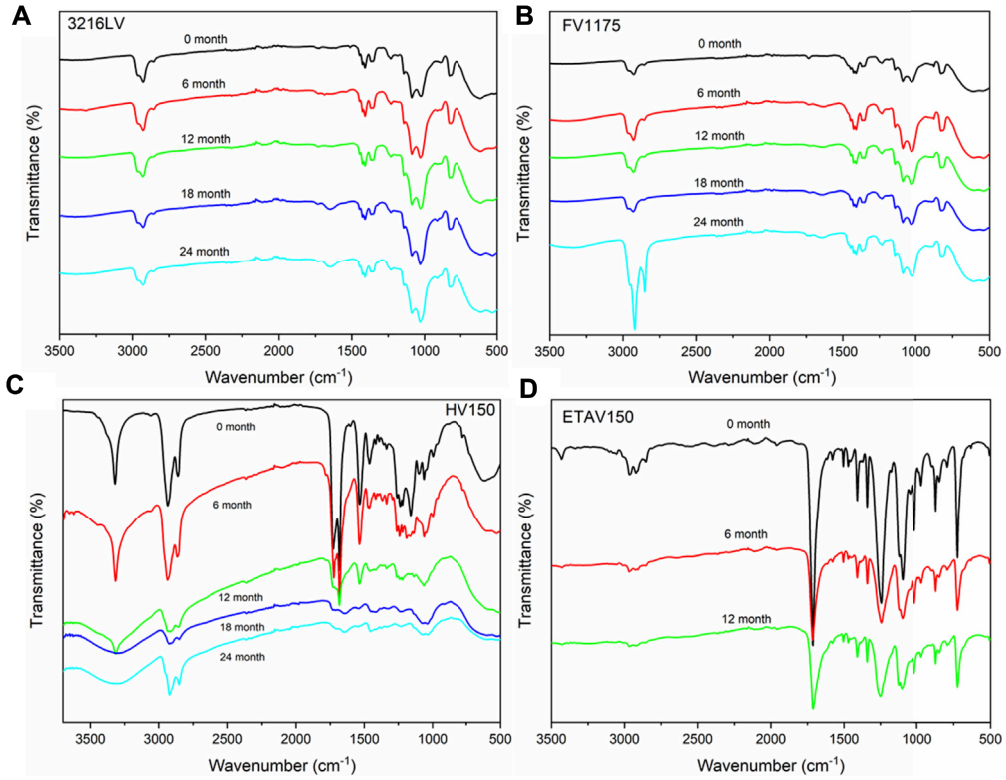

FIGURE 8
FT-IR spectra of **(A)** 3216LV, **(B)** FV1175, **(C)** HV150, and **(D)** ETAV150 before and after natural aging.

Characterizations

The chemical structure of the outer layer for the envelope materials was characterized by VERTEX 70 Fourier Transform-Infra Red Spectroscopy (FT-IR, Bruker, Germany). An Instron 5969 universal testing machine was used to evaluate the mechanical properties at room temperature with a tensile rate of 305 mm/min in a uniaxial test mode according, following the standard Chinese method (GB/T 1040.3-2006). The samples were cut into 25 × 152 mm strips, as shown in Figure 4. At least five specimens of each sample were tested, and the average value was calculated. Tensile strength was defined by ultimate stress at break. The morphology of the samples was obtained by a XL-30 field emission scanning electron microscopy (SEM) under an acceleration voltage of 15 KV with samples gold sprayed before testing. The helium permeability of samples at Φ97 mm was tested at room temperature, using a VAC-V2 gas permeameter (Languang, Jinan) according to Chinese standard method (GB/T 1038-2000). At least three specimens were tested for each sample, and the average value was obtained.

Results and discussions

Morphology of envelope materials

Figure 5 displayed the images of tested envelope materials before and after natural aging. As can be seen, 3216LV showed little change during natural aging, even after being outdoors for 24 months (Figures 5A1–4). Mildew spots appeared in the surface of FV1175 and the size was enlarged with the prolongation of aging time (Figures 5B1–4). The mildew was the most serious, and the surface of HV150 changed from white to gray (Figures 5C1–4) due to the high moisture along the coast and poor water resistance. After aging for 2 years, the surface was all damaged, as shown in Figure 5C4. There were groove marks on the surface of ETAV150, and the marks were more obvious after aging for 12 months (Figures 5D1–3). In particular, the outer layer peeled off at several sites, and the inner layer was exposed, which occupied about one-tenth of the whole surface, as shown in Figure 5D4.

The micro-morphology of samples is given in Figure 6. The original surfaces of 3216LV, FV1175, and ETAV150 were relatively smooth, with few defects (Figures 6A2,B2,D2). Impurities appeared on the surface with the prolongation of

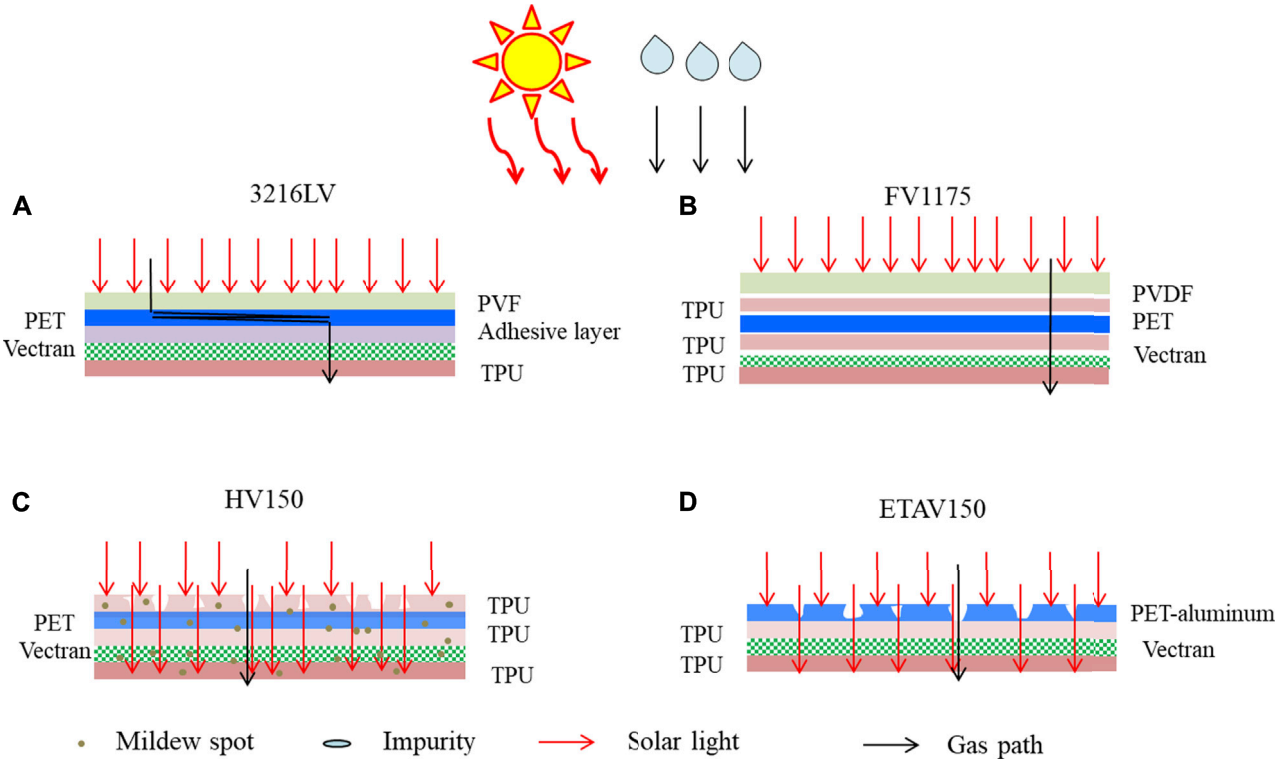

FIGURE 9
Simplified schematic illustration of natural aging mechanism of **(A)** 3216LV, **(B)** FV1175, **(C)** HV150 and **(D)** ETAV150 in Hainan.

aging time, which may be the adherence of dust. In addition, cracks occurred and were extended for ETAV150 after aging for 6 and 12 months (Figures 6D3–4), which indicated breakage of the outer PET-aluminum. The morphology of HV150 clearly changed during natural aging, as shown in Figures 6C1–4. Rough gullies arose with the increase of aging time and the Vectran fabric was exposed after aging for 24 months due to high moisture and severe UV-light irradiation (Duan and Jiang, 2022; Liu et al., 2014). Hence, as can be seen in Figure 6, 3216LV and FV1175 possessed better aging resistance, and ETAV150 and HV150 endured greater damage. For ETAV150, the aluminum was easily corroded in the moist and salty environment (Ul-Hamid, et al., 2017). The outer layer of HV150 was TPU, is was more vulnerable to mildew and was degraded when placed in the environment with such high moisture and irradiation (Duan and Jiang, 2022; Liu et al., 2014) relative to 3216LV and FV1175, whose outer layers were PVF and PVDF film, respectively.

To further estimate the stability of these tested materials, an immersion test was conducted, as follows. Sample pieces were immersed into deionized water and kept for 30 min, and weight before and after immersion was obtained after drying. As can be seen in Figure 7, the water after 3216LV and FV1175 aging for 24 months was as clear as before, and no powder was dissolved. For ETAV150 aging for 12 months, the water was limpid, and some twinkle powders precipitated in the bottom of bottle circled with a red line, which corresponds to the falling off of aluminum. Hence, it could be concluded that the combination of PET-aluminum with other layers was too weak to fall off when rainy. Worse, the water immersing HV150 for 24 months turned muddy, and gray powder sediment appeared, implying poor water-resistance and heavy degradation. The weight change in the envelope materials is listed in Table 2. There was little variation in 3216LV and FV1175, with a 0.01 and 0.11% weight decrease, respectively. However, a 1.96 and 1.36% weight decrease were seen for HV150 and ETAV150, respectively, implying poor water-resistance.

Chemical structure of envelope materials

As shown in Figure 8, the chemical structure of the outer layer for 3216LV and FV1175 showed no change, which implies that the outer layer was relatively stable during natural aging. For HV150, the intensity for -NHCOO- group at 1724 cm^{-1}, the -NHCONH- group at 1680 cm^{-1}, and the C=O group at 1224 cm^{-1} decreased with the increase in natural aging time.

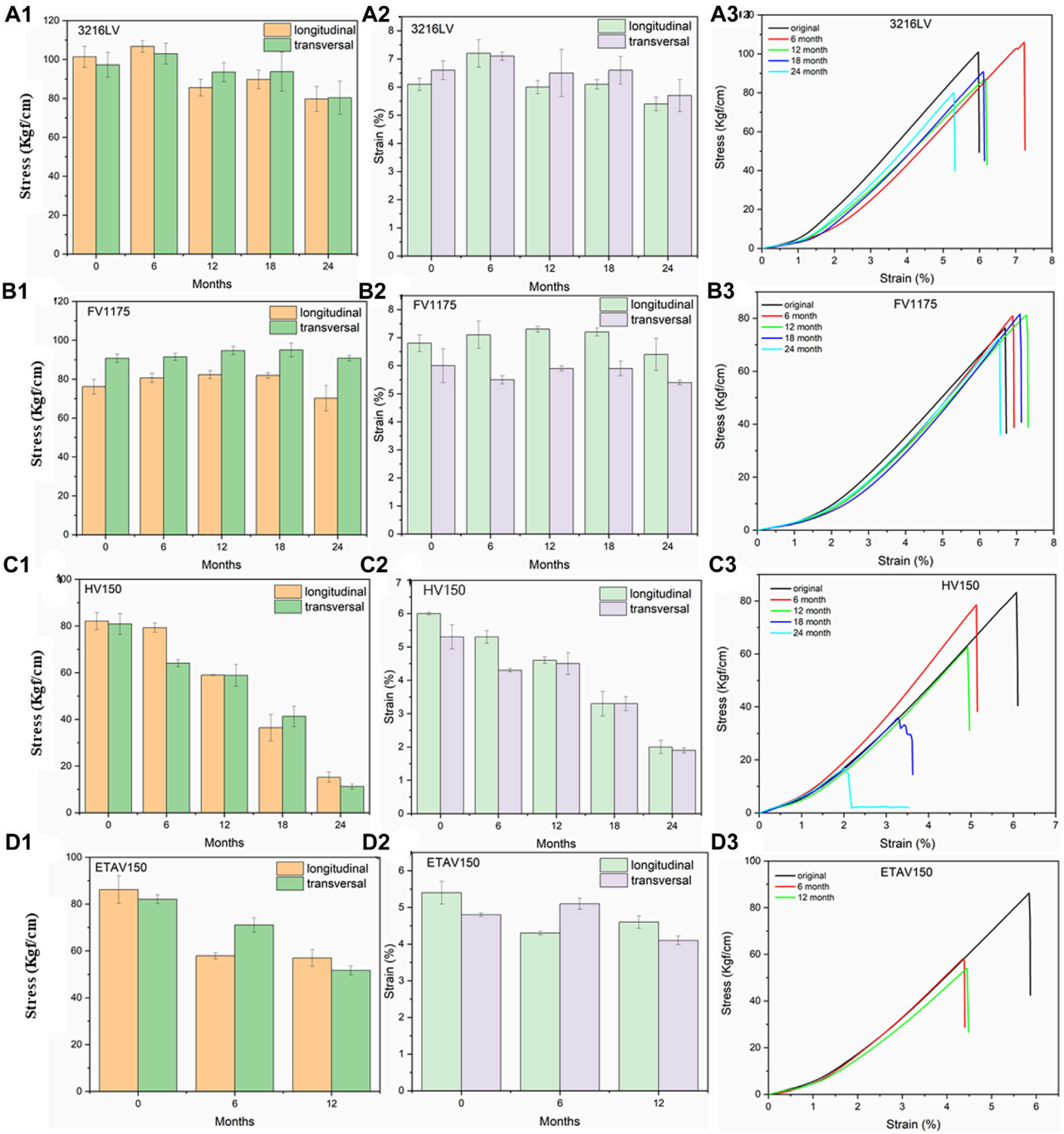

FIGURE 10
Stress-strain curves, bar charts of stress, strain at break and stress-strain curves for **(A1-A4)** 3216LV, **(B1-B4)** FV1175, **(C1-C4)** HV150, and **(D1-D4)** ETAV150.

This result indicated that the outer layer of HV150 was broken during aging, which is consistent with the results shown in Figures 5–7. For ETAV150, the chemical structure showed no change after aging because the tested material chosen was relatively complete without any PET-aluminum fall off.

Helium permeability and mechanical properties of envelope materials

The gas-barrier and mechanical properties of the envelope materials are of vital importance for actual applications. A

TABLE 3 Helium permeability of envelope materials.

Aging months		0	6	12	18	24
Helium permeability (L/m^2•day•atm)	3216LV	0.8818	0.7377	0.9042	0.3776	0.2047
	FV1175	0.6360	0.7233	0.9554	0.2169	leakage
	HV150	0.3658	13.2301	leakage	leakage	leakage
	ETAV150	0.0400	9.0181	leakage	--	--

TABLE 4 Mechanical properties and helium permeability of envelopes aged for different times.

Sample	Aging month	Strength (Kgf/cm)		Strain at break (%)	
		Longitudinal	Transverse	Longitudinal	Transverse
3216LV	0	101.43 ± 5.45	97.31 ± 6.43	6.1 ± 0.22	6.6 ± 0.33
	6	106.75 ± 3.08	103 ± 5.37	7.2 ± 0.49	7.1 ± 0.15
	12	85.57 ± 4.35	93.48 ± 14.85	6 ± 0.23	6.5 ± 0.84
	18	89.75 ± 4.75	93.81 ± 10.09	6.1 ± 0.17	6.6 ± 0.49
	24	79.73 ± 6.40	80.35 ± 11.49	5.4 ± 0.24	5.7 ± 0.57
FV1175	0	76.15 ± 3.81	90.75 ± 2.12	6.8 ± 0.3	6 ± 0.6
	6	80.68 ± 2.40	91.46 ± 1.83	7.1 ± 0.49	5.5 ± 0.15
	12	82.29 ± 2.08	94.71 ± 2.15	7.3 ± 0.1	5.9 ± 0.09
	18	81.90 ± 1.44	95.03 ± 3.58	7.2 ± 0.14	5.9 ± 0.26
	24	70.20 ± 6.57	90.80 ± 1.46	6.4 ± 0.57	5.4 ± 0.08
HV150	0	82.13 ± 3.61	80.87 ± 4.56	6.0 ± 0.04	5.3 ± 0.36
	6	79.29 ± 1.99	64.05 ± 1.52	5.3 ± 0.19	4.3 ± 0.05
	12	58.98 ± 0.13	58.86 ± 4.7	4.6 ± 0.1	4.5 ± 0.33
	18	36.42 ± 5.67	41.30 ± 4.41	3.3 ± 0.37	3.3 ± 0.21
	24	15.22 ± 2.16	11.24 ± 1.01	2.0 ± 0.2	1.9 ± 0.08
ETAV150	0	86.20 ± 5.91	82.07 ± 1.89	5.4 ± 0.31	4.8 ± 0.05
	6	57.92 ± 1.32	71.06 ± 3.03	4.3 ± 0.05	5.1 ± 0.15
	12	56.99 ± 3.57	51.68 ± 1.94	4.6 ± 0.17	4.1 ± 0.12

stratospheric airship would fail if any of these properties did not satisfy application requirements (Liao and Pasternak, 2009). The helium permeability of the samples before and after natural aging was accessed using a differential-pressure method, and the results are listed in Table 3. The helium permeability of the 3216LV declined with the prolongation of aging time from 0.8818 L/m^2•day•atm to 0.2047 L/m^2•day•atm. The helium permeability of the FV1175 increased from 0.6360 L/m^2•day•atm to 0.9554 L/m^2•day•atm when aged for 12 months and decreased to 0.2169 L/m^2•day•atm after aging for 18 months. However, the samples that were aged for 24 months showed leakage due to their stripped-off layers. For HV150 and ETAV150, helium permeability after aging for 6 months jumped from 0.3658 L/m^2•day•atm and 0.0400 L/m^2•day•atm to 13.2301 L/m^2•day•atm and 9.0181 L/m^2•day•atm, which were 36.2 and 225.5 times of the original values, respectively. Later, the samples exhibited leakage.

Thus, the outer layers of HV150 and ETAV150 were broken during natural aging in Hainan. Hence, a surge in helium permeability was seen in ETAV150 due to the corrosion of the PET-aluminum layer when exposed to environment with high moisture and salty, frequent rainfalls (Ul-Hamid, et al., 2017). The aluminum layer was even absent in some areas with obvious cracks in the surface, as shown in Figures 5–7, which provided the decreased gas paths, resulting a failure of gas-barrier layer (Figure 9D). In addition, the degree of damage to HV150 was grave too and exhibited leakage after aging for 12 months. As displayed in Figures 5–7, the mildew spots and area on HV150 were the most apparently and micro-gullies shown on the surface and even Vectran fabrics was exposed, which was harmful to

the performance of HV150. The outer TPU layer was destroyed due to poor water and mildew resistance, leading to the degradation and failure of the weatherability layer. Furthermore, the PET layer suffered solar irradiation and mold erosion, which led to the failure of gas-barrier properties. Finally, the gas path was shortened sharply and showed helium leakage, as shown in Figure 9C. Interestingly, the helium permeability of 3216LV and FV1175 aged for 24 and 18 months, respectively, decreased to a certain extent, which may be ascribed to the crosslinking of the PET part under the comprehensive action of irradiation of ultraviolet light, moisture, and temperature alternation, which could enhance the crystallization degree (Ji-Hyun and Hee, 2018; Shih, et al., 2021; Xu, et al., 2015) and block the diffusion of helium (Figures 9A,B). Meanwhile, the better water and mildew resistance of PVDF and PVF enabled them to have efficient protection of the inner layers, which kept the PET layer working. However, the samples of FV1175 aged for 24 months showed delamination leakage among the layers. It probably was the poor waterability of TPU, which served as the adhesive layer, that led to the delamination, and thus shortening the gas paths, as shown in Figure 9B.

The mechanical properties were tested, and the results are shown in Figure 10 with detailed data listed in Table 4. In 6 months, the tensile strength of 3216LV remained unchanged in both the longitudinal and transverse direction at about 101.43 ± 5.45 Kgf/cm and a strain at break of 6.1 ± 0.22%. With increased of aging time, the strength of 3216LV decreased to 79.73 ± 6.40 Kgf/cm and the strain at break became to 5.4 ± 0.24%, or about a 21.4% and 11.5% decrease, respectively. For FV1175, there was little variation in tensile strength and or strain at break in 18 months. Even after aging for 24 months, the strength and strain decreased form 76.15 ± 3.81 Kgf/cm and 6.8 ± 0.3% to 70.20 ± 6.57 Kgf/cm and 6.4 ± 0.57% in the longitudinal direction. These values remained unchanged in the transverse direction. By contrast, the strength of HV150 and ETAV150 dropped sharply, even after aging for only 6 months. The tensile strength reached 79.29 ± 1.99 Kgf/cm at 6 months and 15.22 ± 2.16 Kgf/cm at 24 months from 82.13 ± 3.61 Kgf/cm, which decreased 3.5 and 81.5%, respectively. The strain at break decreased from 6.0 ± 0.04% to 5.3 ± 0.19% at 6 months and 2.0 ± 0.2% at 24 months, which declined 11.7 and 66.7%, respectively. Meanwhile, ETAV150 also exhibited decreased tensile strength with no sacrifice of strain, with a tensile strength that was maintained 57.92 ± 1.32 Kgf/cm after 6 months aging, 32.8% lower than that of original sample.

Solar irradiation and rainfall affected the performances of these tested materials the most, as illustrated in Figure 8. During natural aging, envelope materials suffered sun irradiation and rainfall with high salt for months and even years. For 3216LV and FV1175, the outer layers were PVF and PVDF with TiO_2, which possess excellent weather resistance and hydrolysis resistance. Hence, the outer layer was stable and protected the inner layers from being broken under solar irradiation and rainfall through reflecting the solar light away and keeping the rainfall out (Figure 9A). As a result, 3216LV and FV1175 remained complete and without defects, contributing to the excellent mechanical properties. For HV150, the hydrolysis and mildew of TPU rendered the degradation of TPU and could not prevent the inner layers from solar light and mildew (Figure 9C). Under these dual actions, the degradation occurred on the Vectran fabrics (Beers and Ramirez, 1990; Said et al., 2006), resulting in a sharp decrease in tensile strength. Similarly, the corrosion of PET-aluminum increased weathering. As a result, solar light could penetrate through the cracks into the inner layer and harm the Vectran, which led to a drop in mechanical properties.

Conclusion

In this work, the properties of several envelope materials for aerostat natural aged in Hainan were investigated. The characteristics of the outer layer were of great importance. The results show that envelope materials employing PVF and PVDF as the weathering layer possessed better aging resistance than TPU and aluminum. The tensile strength of 3216LV using PVF as the outer layer decreased from 101.43 ± 5.45 Kgf/cm to 79.73 ± 6.40 Kgf/cm, even after aging for 24 months, with decreased helium permeability from 0.8818 L/m^2•day•atm to 0.2047 L/m^2•day•atm. The helium permeability of FV1175 decreased from 0.6360 L/m^2•day•atm to 0.2169 L/m^2•day•atm after aging for 18 months, and the mechanical strength was reduced from 76.15 ± 3.81 Kgf/cm to 70.20 ± 6.57 Kgf/cm when aging for 24 months. However, HV150 and ETAV using TPU and PET-aluminum as the outer layer, respectively. showed leakage after aging for 12 months with a sharp drop in mechanical performance. As result, aerostats using 3216LV and FV1175 are more suitable for flying in Hainan.

Data availability statement

The original contributions presented in the study are included in the article/Supplementary material; further inquiries can be directed to the corresponding author.

Author contributions

JL and YZ contributed equally to this work. JL: experiment performance and data collection; YZ: conception and analysis; YZ: supervision; YN and QW: sample preparation and tests. All authors have read and agreed to the submitted version of the manuscript.

Funding

The authors gratefully acknowledge the financial support from the Strategic Priority Research Program of

the Chinese Academy of Sciences, Grant No. XDA26010203.

Conflict of interest

The authors declare that the research was conducted in the absence of any commercial or financial relationships that could be construed as a potential conflict of interest.

Publisher's note

All claims expressed in this article are solely those of the authors and do not necessarily represent those of their affiliated organizations, or those of the publisher, the editors, and the reviewers. Any product that may be evaluated in this article, or claim that may be made by its manufacturer, is not guaranteed or endorsed by the publisher.

References

Baldan, A. (2004). Adhesively-bonded joints and repairs in metallic alloys, polymers and composite materials: Adhesives, adhesion theories and surface pretreatment. *J. Mat. Sci.* 39 (1), 1–49. doi:10.1023/B:JMSC.0000007726.58758.e4

Beers, D. E., and Ramirez, J. E. (1990). Vectran high-performance fibre. *J. Text. Inst.* 81 (4), 561–574. doi:10.1080/00405009008658729

Caldwell, M. M., and Flint, S. D. (1994). Stratospheric ozone reduction, solar UV-B radiation and terrestrial ecosystems. *Clim. Change* 28 (4), 375–394. doi:10.1007/BF01104080

Cicerone, R. J. (1987). Changes in stratospheric ozone. *Science* 237 (4810), 35–42. doi:10.1126/science.237.4810.35

Conrads, P. A., Roehl, E. A., Sexton, C. T., Tufford, D. L., Carbone, G. J., Dow, K., et al. (2010). "Estimating salinity intrusion effects due to climate along the grand of the South Carolina coast," in Joint Federal Interagency Conference 2010: Hydrology and sedimentation for a changing future: existing and emerging issues, Las Vegas, Nevada, June 27 - July 1, 2010.

Duan, J., and Jiang, G. (2022). Synthesis, characterization and properties of antibacterial polyurethanes. *Polymers* 14 (1), 213. doi:10.3390/polym14010213

Gao, X., Sheng, D., Liu, X., Li, T., Ji, F., and Yang, Y. (2016). Tailoring morphology to improve the gas-barrier properties of thermoplastic polyurethane/ethylene-vinyl alcohol blends. *Polym. Eng. Sci.* 56 (8), 922–931. doi:10.1002/pen.24321

Garg, A., Burnwal, S., Pallapothu, A., Alawa, R. S., and Ghosh, A. K. (2011). "Impact of Helium permeability on endurance and altitude control of geostationary stratospheric airship-A mathematical model," in 11th AIAA Aviation Technology, Integration, and Operations (ATIO) Conference, including the AIAA Balloon Systems Conference and 19th AIAA Lighter-Than-air systems technology conference, 20 September 2011-22 September 2011 (Virginia Beach, 6994).

Ji-Hyun, O., and Hee, C. P. (2018). Robust fluorine-free superhydrophobic PET fabric using alkaline hydrolysis and thermal hydrophobic aging process. *Macromol. Mat. Eng.* 303, 1700673. doi:10.1002/mame.201700673

Kang, W., Suh, Y., Woo, K., and Lee, I. (2006). Mechanical property characterization of film-fabric laminate for stratospheric airship envelope. *Compos. Struct.* 75 (1-4), 151–155. doi:10.1016/j.compstruct.2006.04.060

Komatsu, K., Sano, M., and Kakuta, Y. (2003). "Development of high-specific-strength envelope materials," in *AIAA's 3rd annual aviation Technology, integration, and operations* (Denver: ATIO) Forum), 6765. doi:10.2322/jjsass.51.158

Liao, L., and Pasternak, I. (2009). A review of airship structural research and development. *Prog. Aerosp. Sci.* 45 (4-5), 83–96. doi:10.1016/j.paerosci.2009.03.001

Liu, Y., Liu, Y., Liu, S., and Tan, H. (2014). Effect of accelerated xenon lamp aging on the mechanical properties and structure of thermoplastic polyurethane for stratospheric airship envelope. *J. Wuhan. Univ. Technol. -Mat. Sci. Ed.* 29 (6), 1270–1276. doi:10.1007/s11595-014-1080-7

Lv, J., Zhang, Y., Gao, H., and Zhang, T. (2020). Influence of processing and external storage conditions on the performance of envelope materials for stratospheric airships. *Adv. Space Res.* 67 (1), 571–582. doi:10.1016/j.asr.2020.10.016

Meng, J., Cao, S., Qu, Z., Li, J., and Lv, M. (2017). Thermoelasticity of a fabric membrane composite for the stratospheric airship envelope based on multiscale models. *Appl. Compos. Mat.* 24 (1), 209–220. doi:10.1007/s10443-016-9522-3

Meng, J., Lv, M., Tan, D., and Li, P. (2016). Mechanical properties of woven fabric composite for stratospheric airship envelope based on stochastic simulation. *J. Reinf. Plast. Compos.* 35 (19), 1434–1443. doi:10.1177/0731684416652947

Nakadate, M., Maekawa, S., Maeda, T., and Hiyoshi, M. (2009). "Reinforcement of an opening for high strength and light weight envelope material zylon," in 18th AIAA lighter-than-air systems technology conference, Seattle, Washington, 4-7 May 2009, 2853–2859.

Qu, Z., Xiao, H., Lv, M., and Qin, R. (2019). Tear propagation behavior with a novel analytical model on envelope material. *Mat. Res. Express* 6 (10), 105320. doi:10.1088/2053-1591/ab381f

Razak, H. A., Chua, C. S., and Toyoda, H. (2004). Weatherability of coated fabrics as roofing material in tropical environment. *Build. Environ.* 39 (1), 87–92. doi:10.1016/S0360-1323(03)00158-6

Said, M. A., Dingwall, B., Gupta, A., Seyam, A. M., Mock, G., and Theyson, T. (2006). Investigation of ultra violet (UV) resistance for high strength fibers. *Adv. Space Res.* 37 (11), 2052–2058. doi:10.1016/j.asr.2005.04.098

Schäfer, I., Küke, R., and Lindstrand, P. (2002). "Airships as unmanned platforms: Challenge and chance," in 1st UAV Conference, Portsmouth, Virginia, 20 May 2002-23 May 2002, 3423.

Shah, H. N. M., Ab Rashid, M. Z., Kamis, Z., Aras, M. S. M., Ali, N. M., Wasbari, F., et al. (2018). Design and develop an autonomous UAV airship for indoor surveillance and monitoring applications. *JOIV Int. J. Inf. Vis.* 2 (1), 1–7. doi:10.30630/joiv.2.1.33

Shi, T., Chen, W., Gao, C., Hu, J., Zhao, B., Wang, P., et al. (2018). Biaxial strength determination of woven fabric composite for airship structural envelope based on novel specimens. *Compos. Struct.* 184, 1126–1136. doi:10.1016/j.compstruct.2017.10.067

Shih, C. Y., Wang, Y. H., Chen, Y. J., Chen, H. A., and Lin, Y. C. (2021). Enhanced sorption of the UV filter 4-methylbenzylidene camphor on aged PET microplastics from both experimental and theoretical perspectives. *RSC Adv.* 11 (51), 32494–32504. doi:10.1039/D1RA05013C

Tang, J., Duan, D., and Xie, W. (2021). Shape exploration and multidisciplinary optimization method of semirigid nearing space airships. *J. Aircr.* 59, 946–963. doi:10.2514/1.C036684

Tang, J., Wang, X., Duan, D., and Xie, W. (2019). Optimisation and analysis of efficiency for contra-rotating propellers for high-altitude airships. *Aeronaut. J.* 123 (1263), 706–726. doi:10.1017/aer.2019.14

Ul-Hamid, A., Al-Hems, L. M., Quddus, A., Muhammed, A., and Saricimen, U. (2017). Corrosion performance of aluminium in atmospheric, underground and seawater splatter zone in the northeastern coast of Arabian Peninsula. *Anti-Corros. Method. Mat.* 64 (3), 326–334. doi:10.1108/ACMM-05-2016-1677

Vallabh, R., Li, A., Bradford, P. D., Kim, D., and Seyam, A-F. M. (2021). Ultra-lightweight fiber-reinforced envelope material for high-altitude airship. *J. Text. Inst.* 113, 1799–1805. doi:10.1080/00405000.2021.1948695

Wang, F., Chen, Y., Xu, W., Song, Z., and Fu, G. (2017). Experimental study on uniaxial tensile and welding performance of a new coated fabric for airship envelopes. *J. Ind. Text.* 46 (7), 1474–1497. doi:10.1177/1528083715627164

Wrobel, F., Vaille, J. R., Pantel, D., Dilillo, L., Rech, P., Galliere, J. M., et al. (2011). Experimental characterization of an atmospheric environment with a stratospheric balloon. *IEEE Trans. Nucl. Sci.* 58 (3), 945–951. doi:10.1109/TNS.2011.2136359

Xu, Y. J., Song, Y. H., and Zheng, Q. (2015). Effects of nanosilica on crystallization and thermal ageing behaviors of polyethylene terephthalate. *Chin. J. Polym. Sci.* 33, 697–708. doi:10.1007/s10118-015-1619-x

Zhai, H., and Euler, A. (2005). "Material challenges for lighter-than-air systems in high altitude applications," in AIAA 5th ATIO and 16th Lighter-Than-Air Systems Technology and Balloon Systems Conferences, Arlington, Virginia, 26 September 2005, 7488.